JOURNAL OF MATERIALS SCIENCE 40 (2005) 5757–5762

Hot deformation and processing map of 15%SiC_p/2009 Al composite

B. L. XIAO*, J. Z. FAN, X. F. TIAN, W. Y. ZHANG, L. K. SHI
National Engineering Research Center for Non-Ferrous Metal Composites, General Research Institute for Nonferrous Metals, Beijing 100088, People's Republic of China
E-mail: xiaobolv@163.com

Published online: 25 August 2005

Hot deformation characteristics of a 15 vol% SiC_p/2009 Al composite fabricated by powder metallurgy were studied by compressive tests conducted at strain rates of 0.001 to 10 s^{-1} and temperatures of 350 to 500°C. A processing map on basis of a Dynamic Material Model was generated. Different deformation mechanisms such as dynamic recrystallisation (DRX) and superplasticity interpreted by processing map were validated by microstructure observation. Adiabatic shear band formation was observed at higher strain rates, thereby defining the flow instability domain.

1. Introduction

Aluminum matrix composites (AMC) reinforced with stiff ceramic particulate are recognized as an important advanced material owing to their desirable properties, such as low density, high specific stiffness or strength, low thermal expansion, superior dimension stability, increased fatigue resistance, and availability of cheaper reinforcement and comparatively low cost, high volume production methods [1–3]. However, the ceramic particulates restrict plastic flow of matrix alloy leading to relative poor formability of composites compared with that of unreinforced alloys, such as rolling, forging as well as extrusion. Proper selection of forming parameters (including forming temperature and speed represented by strain rate) critically affects the production of sound components, which requires abundant experiment data and numerical models. Hot workability of conventionally produced (i.e., ingot metallurgy) AMCs and alloys has been extensively evaluated in the past years [4–11], however, limited studies have reported on the hot deformation behavior and processing parameters of powder metallurgy (PM) AMCs and alloys [12–16]. It is hard to evaluate workability of composites fabricated by PM, considering that hot deformation characteristics of PM aluminum alloy and AMCs are quite different from those of similar casting materials.

The present work is, therefore, in an attempt to study the hot working behaviors and the effect of hot deformation on microstructure of a PM 2009 Al reinforced with 15 vol% silicon carbide particulate. Processing map based on a Dynamic Material Model [17, 18] was generated as an explicit representation of the response of composites in terms of microstructure mechanism.

2. Experimental procedure

The present composite containing 15 vol pct silicon carbide particulate was fabricated through powder metallurgy route. A 2009 Al powder with an average diameter of 30 μm and α-SiC particulate with a nominal size of 10 μm were initially mixed in a biaxis rotary mixer, and subsequently cold compacted. The as-compacted green billet was degassed and consolidated at 550°C, followed by hot extruded at 450°C with a ratio of 15:1.

Cylindrical specimens with 8 mm in diameter and 12 mm in height for compressive tests were machined from as extrude bar with the axis of specimens parallel to extrusion direction. Uniaxial hot compressive tests were conducted on Gleeble 3500 to achieve a constant strain rate deformation. Specimens were heated to test temperatures, soaked for 10 min for equilibration. Fluctuation of temperature was controlled within ±1°C. The specimens were compressed with a height reduction of 42%, in isothermal condition at the temperature and strain rate ranges of 350–500°C and 0.001–10 s^{-1}, respectively. The compression direction was parallel with axis of specimens. Deformed specimens were air quenched and sectioned parallel to the compression axis, the cut surface was prepared for microstructure examination by standard optical and scanning electron microscopy techniques.

3. Experimental results and discussion

3.1. Initial microstructure

Fig. 1 represents the micrograph of as-extruded 15% SiCp/2009 Al composite. It reveals fine equiaxed recrystallized grain structure formed out of the original grains elongated in the extrusion direction due to

*Author to whom all correspondence should be addressed.
0022-2461
DOI: 10.1007/s10853-005-1292-5

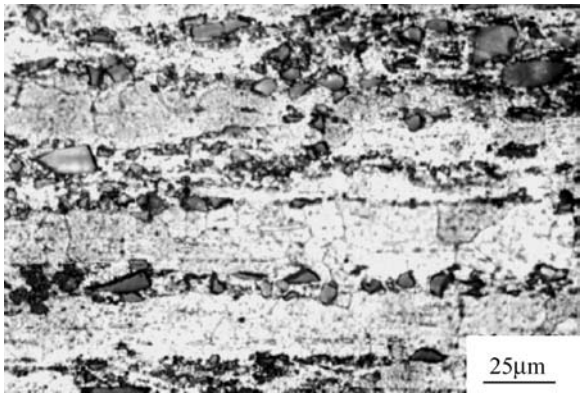

Figure 1 Optical micrograph of as extruded 15%SiCp/2009 Al.

anneal during hot extrusion. Similar results were shown in the observation of Radhakrishna Bhat *et al.* [16]. The average grain size is about 13 μm. The coarser grain size may be attributed to the lower extrusion ratio (15:1).

3.2. Flow curves

Typical flow curves (for 450°C and each test strain rate) are shown in Fig. 2a. The flow stress rises with increase of the strain rate. A maximum flow stress value followed with flow softening is observed at higher strain rates while it is absent at strain rates below 0.1 s^{-1}. Deformation at higher strain rates is almost adiabatic as consequence of the inadequate heat transmission due to insufficient durations. In addition, lower rate of dislocation generation at higher strain increases the dynamic yield stress. This lead to a peak stress value and flow softening. Further, a fluctuant curve at comparatively high strain rate (>0.1 s^{-1}) is observed in Fig. 2a, the same phenomenon is shown in Fig. 2b at each test temperature. These results indicate that flow softening behavior occurs in matrix. Traditional dynamic recrystallisation (DRX) occurs in low stacking fault energy (SFE) metals during hot deformation. Prasad and Seshacharyulu [19] opined that recrystallinsation did not occur in aluminum in view of its high SFE and the primary softening mechanism was only dynamic recovery except for high pure aluminum and some particle containing alloys. However, many authors demonstrated that DRX was more likely to occur due to high-density dislocation formed by addition of a large fraction of hard particle. Recently, Garnesan *et al.* [20] indicated that flow stress curves corresponding to DRX region of processing map did oscillate. It can be inferred that DRX is likely to occur in present composites. The oscillations of flow curves may be attributed to insufficient strain values in present test before achieving steady state. These would be discussed later with observation of microstructure.

An early attempt [21] to evaluate the mechanisms of hot working, that is, the steady flow stress in hot deformation is related to strain rate and temperature by Arrhenius relationship:

$$\dot{\varepsilon} = A\sigma^n \exp(-Q/RT) \tag{1}$$

where $\dot{\varepsilon}$ is the strain rate, A the constant, σ the steady flow stress, n stress component, Q the activation energy, R the gas constant and T is the absolute temperature. An effective stress equal to difference between applied stress and threshold stress may substitute the flow stress σ. On the basis of an apparent energy, deformation mechanisms may be evaluated and microstructure correlations obtained with a temperature compensation strain rate parameter, Z defined as:

$$Z = \dot{\varepsilon}/A \exp(Q/RT) = \sigma^n \tag{2}$$

The kinetic analysis is applicable for pure metals and dilute alloys but when extended to commercial alloys and AMC with complex microstructures, the apparent activation energy values become too complex to interpret in terms of a single mechanism [22]. In addition, tests at very low strain rates are absent. It is hard to calculate values of threshold stress. Thus, a processing map is generated for understanding the response of the composite to deformation.

3.3. Processing maps

A processing map is obtained by superimposition of the variation of the efficiency of forming parameter with temperature and strain rate and the variation of instability parameter as a function of the same variables. The approach follows the Dynamic Material Model [17, 18]

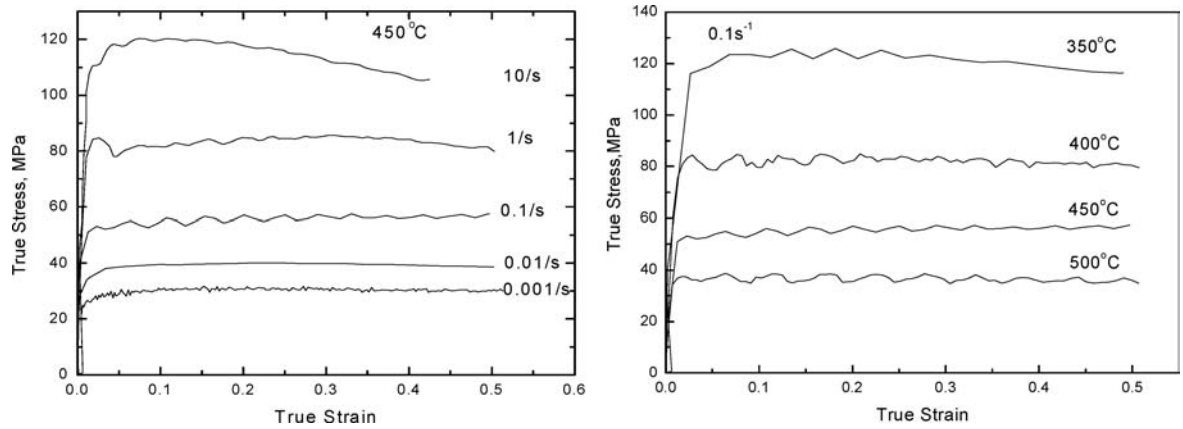

Figure 2 Flow stress curves at (a) variation strain rate (b) variation temperature.

that considers the machine as a source of power and the material as a power dissipator. The power dissipation maps are continuum maps and are interpreted in terms of the microstructural processes making use of the ideas discussed in the processing maps reported earlier by Gandhi and Raj [23–25], which are developed on the basis of an atomistic approach. These maps reveal the limiting temperature and strain rate conditions for the occurrence of fracture and instability processes. For metal matrix composites, voids usually form at interfaces when deformed at lower temperatures and higher strain rates [20, 22], whereas wedge cracking occurs at grain boundary triple junctions at higher temperatures and lower strain rates. Flow instability is likely to occur at very high strain rates, typically represented by the formation of adiabatic shear band (ASB). The flow of metal matrix composites is controlled by two main processes [26]: the transfer of load from ductile matrix to hard particles and the microstructural transformations such as recrystallization or damage phenomena; in this case the material can present decohesion at matrix–particles interfaces or several particle cracking. When the material is able to dissipate applied power through the load transfer or through metallurgical transformations, it does not reach high levels of damage [27–29]. A processing map gives safe "processing windows" [22] in which the processes of dynamic recovery and DRX occur. Dynamic recovery and DRX are main mechanism of flow softening to keep flow stresses and rates of work hardening considerably low [25]. Although these maps give the general guidelines, the interpretation of domains in the map will have to be microstructurally validated.

In this study, processing map based on Dynamic Materials Model [17, 18] is generated by the procedure as follows: flow stress values are corrected for adiabatic temperature rise during testing, using log σ vs. $1/T$ plots at constant strain rate. The flow stress values at intermediate temperatures are obtained by linear interpolation from the same plots. The log σ vs. log $\dot{\varepsilon}$ data at a constant temperature and strain are fitted using a cubic spline, and the strain rate sensitivity m is calculated as function of strain rate at each temperature. The efficiency of power dissipation through microstructure changes [22],

$$\eta = 2m/(m+1) \tag{3}$$

is then calculated from values of m at constant strain. A dimensionless parameter denoted by $\xi(\dot{\varepsilon})$, given by

$$\xi(\dot{\varepsilon}) = \frac{\partial \ln\left(\frac{m}{m+1}\right)}{\partial \ln \dot{\varepsilon}} + m > 0 \tag{4}$$

is used to be criteria for obtaining instability map.

Typical processing maps generated using the preceding test data at a strain of 0.3 and 0.5 are presented in Fig. 3a and b. The contour numbers represent power dissipation efficiency and the shaded domains indicate the regions of flow instability. No obvious differences are observed in both of maps except for the efficiency slightly increasing with the true strain.

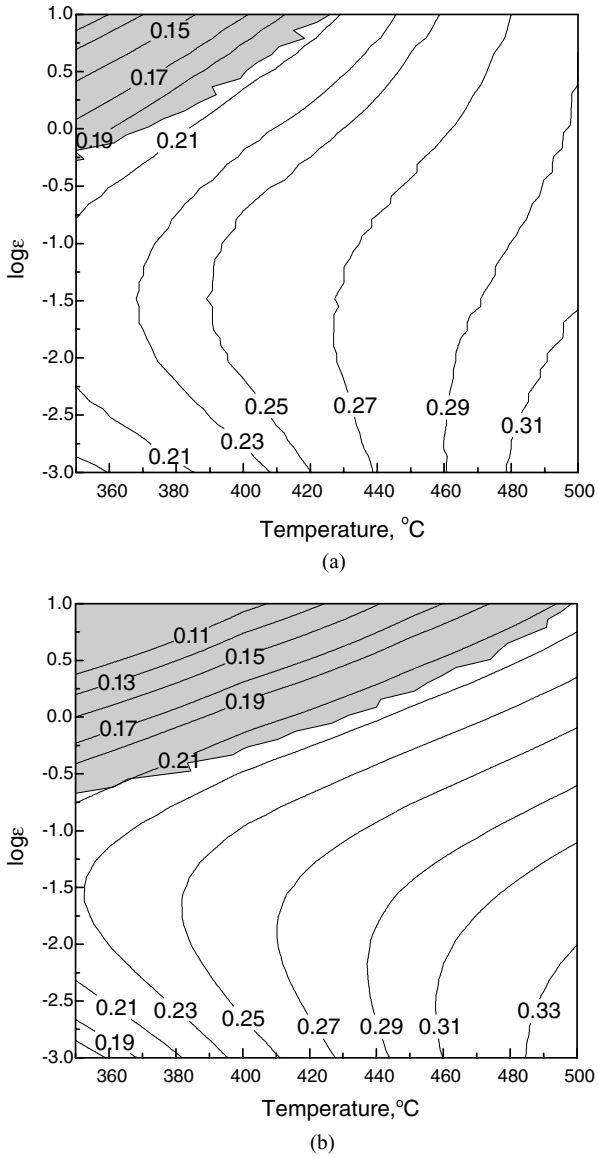

Figure 3 Processing map at strain of (a) 0.3, and (b) 0.5.

The map at strain of 0.5 can be divided into three main regions. The first region is in top left corner of the map and is almost superimposed with the instability region. There is a steep hill of efficiency that increases from 0.11 to 0.21. It implies a damage process that interfacial crack occurs and the energy dissipation increase is through the formation of new surfaces [20]. In this study, no obvious crack in grain boundaries or interfaces is observed. However, flow instability like ASB is found in specimen tested at 350–500°C and strain rate from 0.3 to 10 s^{-1}, as shown in Fig. 4. Thus, this region of parameters corresponding to flow instability is undesirable for processing and hence should be avoided.

The second region is in midst of the map having the maximum efficiency of 0.31 increasing from 0.23. The flow stress curves show oscillation at higher temperatures (400–450°C) and strain rates (>0.01 s^{-1}). The microstructure of specimens is shown in Fig. 5 with the structure having the three features as followed: (1) equiaxed grain formed in the band structure by extrusion, (2) grain size is fine (about 7 μm) compared with initial grain size (as extruded), it is indicative of

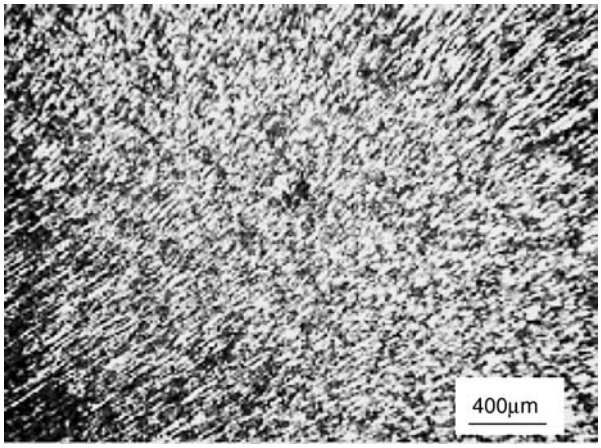

Figure 4 Microstructure of specimen tested in 350°C and 10 s^{-1}.

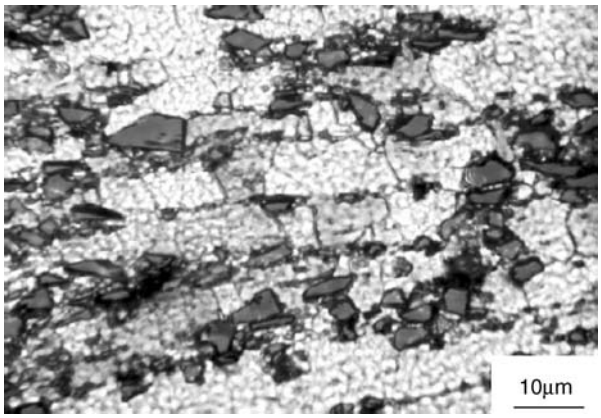

Figure 5 Microstructure of specimen tested in 450°C and 0.1 s^{-1}.

refinement of grain, and (3) grain boundaries are irregular or wavy in nature. These features agree well with DRX [22]. Moreover, high-density dislocation and developed subgrain in the vicinity of SiC particles were found through transmission electron microscopy (TEM) as shown in Fig. 6. It is well known that during the deformation of composites, enforced strain gradient in the vicinity of a non-deforming particle creates a region of high dislocation density and large orientation gradient, which is an ideal site for the development of a recrystallisation nucleus [28]. Further, subgrain boundaries formed by dynamic recovery progressively transform at large strains into new high angle grain boundaries [30]. At a critical strain, which is a function of the flow stress and the initial grain size, the spacing of the high-angle boundaries is reduced to the dimensions of the subgrain size, the high angle boundaries begin to touch with each other and a new microstructure of mainly high angle boundaries is effectively formed [31–33] and evolve into a very fine grain structure classified as "continuous recrystallization" [30]. Many authors have widely confirmed that the addition of ceramic reinforcements to aluminum alloys promoted the initiation of DRX during hot deformation by increasing dislocation density in the matrix [15, 34]. It had also been proven that during hot deformation, DRX indeed occurred in AMC whether fabricated by cast or PM method. Grain refinement by DRX is advantageous for improvement of mechanical properties especial for cast composite usually having coarse grain microstructure. However, the critical strain (at which DRX occurs) as mentioned previously maybe different for casting and PM composites. It can be found in Fig. 2b that the oscillations of flow curves appear at initial stage (about strain value of 0.1). The result indicates that DRX occurs at lower strain. Compared with casting composites, many nano-scale oxide particles have been incorporated in PM composites during fabrication process. These particles pinning up dislocation during hot deformation decreases the restoration rate. It results in higher dislocation density at a certain strain (assumed the reinforcement and initial grain size of two kinds of composites were same). DRX instead of dynamic restoration hereby occurs with high driven force. The critical strain of DRX for present composite is thus lower than that of casting composites reported by other authors [22].

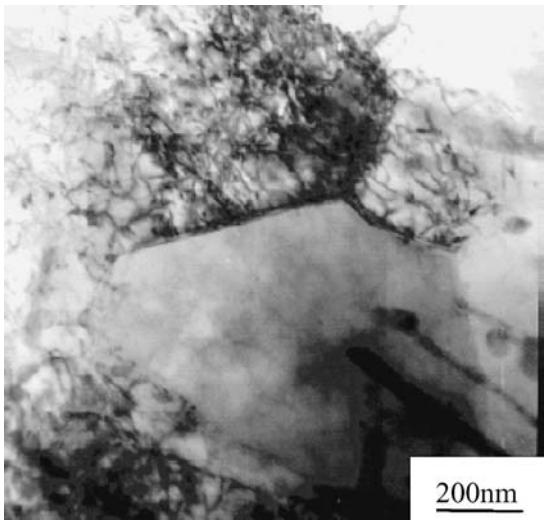

Figure 6 TEM micorgraph of specimen tested in 400°C and 0.1 s^{-1}.

Another notable feature in Fig. 5 is that the equiaxed grains are fine even in SiC_p free region. However, the status is quite different at 500°C and 10 s^{-1} while values of efficiency keep same moderate. Coarse grain is found especially in the particle free region (Fig. 7). Compared with high strain rate, density of dislocation is relatively uniform at moderate strain rate. In addition, the precipitation as well as oxide particles in matrix of PM materials that plays an important role in creep deformation is helpful for increasing the density hence the recrystallisation occurs in the particle-free region. During hot deformation of composites at high strain rates, temperature has been raised by insufficient heat transmission compared with that at low strain rate. As the result, flow localization occurs leading to the formation of non-uniform slip band even ASB while the non-uniformity may be expanded with the non-uniform distribution of SiC particle. Moreover, the generation rate of dislocation is comparatively low during work hardening stage. Thus, the density of dislocation may be lower than that at low strain rate in the region of particle free region. The above factors will reduce the nucleation hence subsequent recrystallisation thus is inadequate. Further, precipitation particles

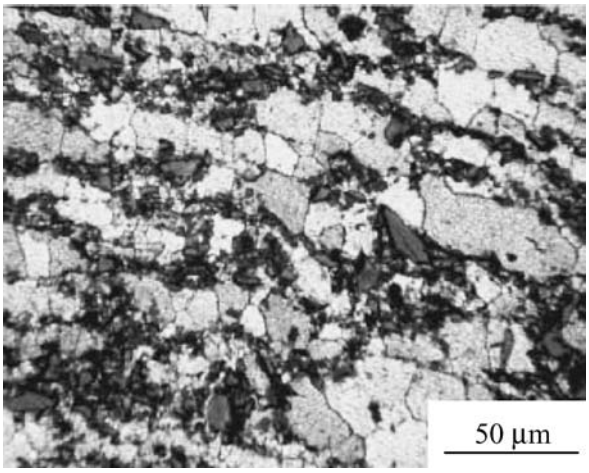

Figure 7 Microstructure of specimen tested in 500°C and 10 s^{-1}.

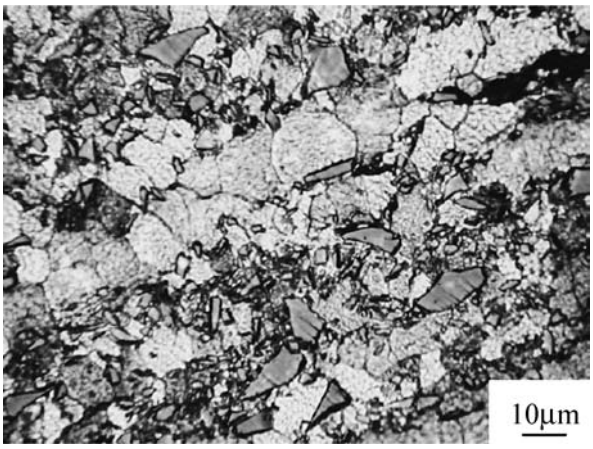

Figure 8 Microstructure of specimen tested in 500°C and 0.001 s^{-1}.

may dissolve or coarsen in the matrix due to increase of temperature by deformation besides test temperature. The grain boundaries migration therefore promotes growth of grain without fine particles effectively pinning grain boundaries.

The third region is in bottom right corner of the map corresponding to the highest temperature and lowest strain rate, in which (1) the flow curves are smooth and flow stress is low, (2) value of efficiency is highest, (3) gain size is close to initial size (Fig. 8). Further, an alternate test with load axis perpendicular with extrusion direction at same temperature and strain rate shows a diamond configuration in grain shape. The result is indication of grain boundaries sliding. These features agree well with that of superplastic deformation [22, 35]. PM alloys and composites with fine initial grain size exhibit abnormal high elongation rate in tension at higher temperatures and strain rates than traditional casting metals. A tensile test of present composite shows a elongation of 30% at 500°C and an initial strain rate of 0.0005 s^{-1}. The strain rate of superplastic deformation for the tensile test seems to be lower than that of other superplastic PM composites [35, 36]. In fact, (1) the strain rates corresponding to maximum superplastic elongation increase with decrease of initial grain size, (2) elongation rate decreases large if wedge crack occurs [22]. The wedge crack due to low rate of diffusion at the grain boundaries triple junctions during grain boundaries sliding (GBS) could be prevented by reducing GBS. Coarse grain or high strain rate and low temperature can effectively lower GBS. Therefore, fine grain alloy and metal matrix composites fabricated by PM can be processed at high strain rate by superplastic deformation. It is benefit for mass production of component. For aluminum matrix composite, mechanism of superplastic deformation is main GBS. Flow softening in superplastic deformation region of processing map is resulted from GBS instead of DRX. Thus obvious grain refinement is absent at superplastic deformation condition. In other words, secondary processing at the case can hardly refine coarse grain by primary processing. Detailed microstructure investigation on superplasticity of present composites should be conducted in future work.

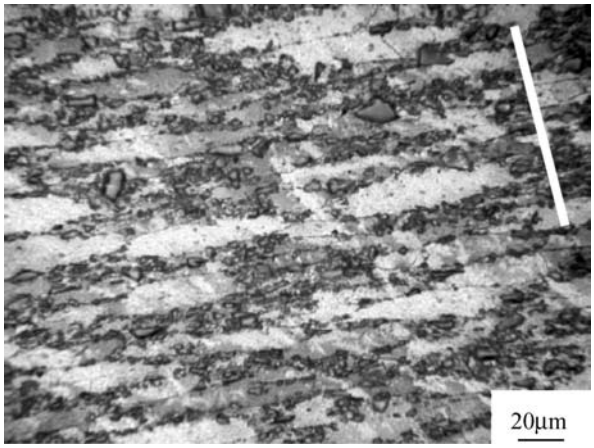

Figure 9 Microstructure of specimen tested in 500 and °C and 0.001 s^{-1} (compress axis parallel to normal of extrusion direction)

4. Conclusion

The hot working characteristics of a 15 vol% SiCp/2009 Al composites were identified by processing map based on a Dynamic Materials Model with microstructure validation. Dynamic recrystallisation occurred at moderate values of dissipation efficiency (except for flow instability) in processing map leading to flow softening. At higher temperature (~500°C) and lower strain rate (0.001 s^{-1}) corresponding to highest value of efficiency, superplastic deformation occurred.

References

1. W. H. HUNT, *J. Met.* **45** (1993) 18.
2. J. E. ALLISON and G. S. COLE, *ibid.* **45** (1993) 19.
3. M. G. MCKIMPSON, E. L. POHLENZ and S. R. THOMPSON, *ibid.* **45** (19 93) 26.
4. H. J. MCQUEEN and J. J. JONAS, in "Metal Forming: Interrelation between Theory and Practice" edited by A. L. Hoffmanner (Plenum Publ Corp, New York, 1971) p. 393.
5. H. J. MCQUEEN and E. EVANGELISTA, N. JIN and M. E. KASSNER, *Metall. Mater. Trans. A* **26A** (1995) 1757.
6. H. J. MCQUEEN, E. EVANGELISTA and M. E. KASSNER, *Z. Metallkde.* **82** (1995) 336.

7. E. EVANGELISTA, F. GABRIELLI, P. MENGUCCI and E. QUADRINI, in, "Strength of Metals and Alloys" edited by P. O. Kettunen, T. K. Lepisto and M. E. Lehtonen (Pergamon Press, Oxford, UK, 1988) p. 977.
8. E. EVANGELISTA, E. DIRUSSO, H. J. MCQUEEN and P. MENGUCCI, in, Homogenization and Annealing of Aluminium and Copper Alloys, edited by H. D. Merchant, J. Crane and E. H. Chia(The Minerals, Metals and Material Society, Warrendale, PA, 1988) p. 209.
9. H. J. MCQUEEN, in: edited by T. G. Langdon, H. D. Merchant, J. G. Morris, and M. A. Zaidi, "Hot Deformation of Aluminum Alloys", (The Minerals, Metals and Material Society, Warrendale, PA, 1991) p. 31.
10. H. J. MCQUEEN, in, "Hot Deformation of Aluminum Alloys", edited by T. G. Langdon, H. D. Merchant, J. G. Morris and M. A. Zaidi (The Minerals, Metals and Material Society, Warrendale, PA, 1991) p. 105.
11. H. J. MCQUEEN, J. J. JONAS, *Mater. Sci. Eng.* **A322** (2002) 43.
12. E. EVANGELISTA, A. FORCELLESE, F. GABRIELLI and P. MENGUCCI, in "HotDeformation of Aluminium Alloys" edited by T. G. Langdon, H. D. Merchant, J. G. Morris and M. A. Zaidi (The Minerals, Metals and Material Society, Warrendale, PA, 1991) p. 121.
13. E. CERRI, E. EVANGELISTA, A. FORCELLESE, P. FIORINI and J. STOBRAWA, in "Strength of Metals and Alloys" edited by H. Oikawa et al. (The Japan Institute of Metals, Tokyo, 1994) p. 807.
14. F. BARDI, M. CABIBBO, E. EVANGELISTA, S. SPIGARELLI and M. VUKČEVIČ, *Mater. Sci. Eng. A* **339** (2003) 43.
15. B. C. KO and Y. C. YOO, *J. Mater. Sci.* **35** (2000) 4073.
16. B. V. RADHAKRISHNA BHAT, Y. R. MAHAJAN and Y. V. R. K. PRASAD, *Metall. Mater. Trans. A* **31A** (2000) 629.
17. Y. V. R. K. PRASAD, H. L. GEGEL, S. M. DORAIVELU, J. C. MALAS, J. T. MORGAN, L. A. LARK and D. R. BARKER, *Metall. Trans. A* **15A** (1984) 1883.
18. H. L. GEGEL, J. C. MALAS, S. M. DORAIVELU and V. A. SHENDE, "Metals Handbook", 9th edn., (ASM, Metals Park, OH, 1988) p. 417.
19. Y. V. R. K. PRASAD and T. SESHACHARYALU, *Int. Mater. Rev.* **43** (1998) 243.
20. G. GANESAN, K. RAGHUKANDAN, R. KARTHIKEYAN and B. C. PAI, *Mater. Sci. Eng. A* **369** (2004) 230.
21. J. J. JONAS, C. M. SELLARS and W. J. MCG. TEGART, *Met. Rev.* **14** (1969) 1.
22. Y. V. R. K. PRASAD and S. SASIDHARA, "Hot Working Guide A Compendium of Processing Maps", (ASM International, Materials Park, OH) p. 3.
23. C. GANDHI and R. RAJ, *Metall. Trans. A* **12A** (1981) 515.
24. R. RAJ, *ibid.* **12A** (1981) 1089.
25. C. GANDHI, *ibid.* **13A** (1982) 1233.
26. P. CAVALIERE, E. CERRI and P. LEO, *Comp. Sci. Tech.* **64** (2004) 1287.
27. A. L. HOFFMANNER, "The Use of Workability Test Results to Predict Processing Limits, Metal Forming: Interrelation between Theory and Practice". (Plenum Press, New York, 1961) p. 349–391.
28. F. J. HUMPHREYS and M. HATHERLY "Recrystallization and related annealing phenomena". (Elsevier, Amsterdam, 1995).
29. S. L. SEMIATIN, J. J. JONAS "Formability and Workability of Metals: Plastic Instability and Flow Localization". (ASM Metals Park, OH, 1984). p. 156.
30. P. CAVALIERE, *Compo. Part A* **35** (2004) 619.
31. H. J. MCQUEEN, E. EVANGELISTA, J. BOWLES and G. CRAWFORD, *Met. Sci.* **18** (1984) 395.
32. F. J. HUMPHREYS, *Acta Mater.* **45** (1997) 4231.
33. S. GOURDET and F. MONTHEILLET. *ibid.* **50** (2002) 2801.
34. Y. C. YOO, J. S. JEON and H. I. LEE, *Comp. Sci. Technol.* **57** (1997) 651.
35. Y. LI and T. G. LANGDON, *Acta Mater.* **46** (1998) 1143.
36. W. J. KIM and O. D. SHERBY, *ibid.* **48** (2000) 1763.

Received 18 September 2004
and accepted 31 March 2005